ACS APPLIED MATERIALS & INTERFACES

Article

Free-energy-driven lock/open assembly based optical DNA sensor for cancer-related microRNA detection with a shortened time-to-result

Xiyu Zhu, Ruoyu Wang, Xiaohong Zhou, and Hanchang Shi

ACS Appl. Mater. Interfaces, **Just Accepted Manuscript** • DOI: 10.1021/acsami.7b06579 • Publication Date (Web): 14 Jul 2017

ACS Publications

ACS Applied Materials & Interfaces is published by the American Chemical Society.
1155 Sixteenth Street N.W., Washington, DC 20036

Free-energy-driven lock/open assembly based optical DNA sensor for cancer-related microRNA detection with a shortened time-to-result

Xiyu Zhu,[§] Ruoyu Wang,[§] Xiaohong Zhou and Hanchang Shi*

State Key Joint Laboratory of ESPC; Center for Sensor Technology of Environment and Health, School of Environment, Tsinghua University, Beijing 100084, China.

Keywords: microRNA detection; free-energy-driven; dynamic locker; evanescent wave; fiber based biosensor.

Abstract: Quantification of cancer biomarker microRNAs (miRs) by exquisitely designed biosensors with a short time-to-result is of great clinical significance. With immobilized capture probes (CPs) and fluorescent labeled signal probes (SPs), surface involved sandwich-type (SST) biosensors serve as powerful tools for rapid, highly sensitive and selective detection of miR in complex matrices as opposed to the conventional techniques. One key challenge for such SST biosensors is the existence of false negative signals when the amount of miRs exceeds SPs in solution phase for a surface with limited number of CP. To meet this challenge, a dynamic lock/open DNA assembly was designed to rationally program miR/SP hybrids pathway. Based on secondary structure analysis and free energy assessment, a "locker" strand that partially hybridize with target miR by two separated short arms was designed to stabilize target miR, preventing possible false negative signals. The strategy was demonstrated on a fiber based fluorescent DNA sensing platform. CP/miR/SP sandwiches formed on the fiber surface would generate fluorescent signals for

quantitatively analysis. The developed SST biosensor was able to detect miR Hsa *let-7a* with a detection limit of 24 pM. The applicability of this free-energy-driven lock/open assembly based optical DNA sensor was further confirmed with spiked human urine and serum samples.

Introduction

Accurate methods for early cancer diagnosis are urgently needed in clinical applications. One promising solution is to detect emerging cancer biomarkers by exquisitely designed biosensors.[1] MicroRNA (miR) is small non-coding RNA whose aberrant expression correlates with disease and stress states. In the past decade, miRs have been reported to have close relationship with various human cancers.[2] An online miR-cancer association database (miRCancer) has been established, which currently documents more than 5000 miR-cancer relationships.[3] Following this trend, the use of miRs as cancer indicators in clinical diagnosis or as suppressors for treatment purposes holds vast potential.

Traditional miR detection relies on amplification-based molecular techniques using polymerase and microarray.[4] Sample preparation (isolation, pre-concentration and labeling) could be a crucial step for the ultimate analytical performances of such assays. Besides, the high sequence homology, easy degradability and low intracellular expression levels hinder the further application of such conventional methods.[5] Moreover, microarray detection method relies on the end-point hybridization intensity, which may lead to a biased result.[6]

Recently, miR biosensors have presented an attractive alternative to traditional techniques, offering highly sensitive analysis in complex physiological matrices with a shortened time-to-result (TTR).[4] In general, miR biosensors can be classified as either labeled or label-free sensors according to the

sensing mechanism. In both cases, linear DNA probes of complementary sequence to the target miR are immobilized on a functionalized transducer surface as typical biorecognition elements. Hybridized miRs could be directly detected by label-free techniques, such as surface plasmon resonance (SPR),[6] arrays of silicon photonic microring resonators[7] and silicon nanowire biosensors.[8] Although label-free biosensors exhibit concise design and facile preparations, the major challenge for miR detection using conventional label free technique is the inability to measure extremely small changes in refractive index, which hinders its application in ultrasensitive detection.[9] Besides, some label free techniques are reported to suffer from severe non-specific adsorption of proteins, which may hinder their further applications in clinical detections.[10-11]

On the other hand, labeled method relies on a signal reporter (such as organic dyes, quantum dots, electrochemical redox reporters and other functional nanomaterials) to generate readable signals corresponding to the amount of bound targets. From a practical point of view, the most widely used labeled scheme is the sandwich assay, which requires two probes that bind to different regions of the target. The classic enzyme-linked immunosorbent assay (ELISA) could serve as a canonical example of a sandwich assay.[12] Recently, a number of sandwich type biosensors have been developed for miR detection based on colorimetric,[13] electrochemical[14] and fluorescent[15] sensing modes. The underlying principle is based on sandwich-type of "signal probe DNA/miR/capture probe DNA (SP/miR/CP)" hybridization reaction (case 1, Figure 1).

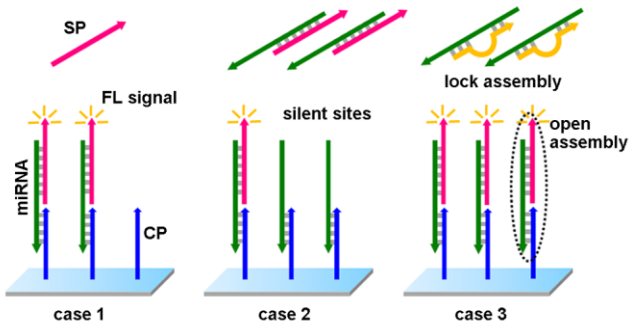

Figure 1. Three possible cases for a surface-involved sandwich-type (SST) miR biosensor.

However, surface-involved sandwich-type (SST) biosensors with a limited number of capture probes (CPs) may suffer from false negative signals when the amount of target miR is more than signal probes (SPs) (case 2, Figure 1). As shown in case 2, free miR strands and miR/SP hybrids compete for limited surface hybridization sites, causing silent CP/miR sites that are unable to produce signals. One way to avoid this problem is to increase the amount of SP. For example, in the work of Wen and co-authors, the molar ratio of biotinylated SP to target miR is more than 500:1 (5 μM of biotinylated SP were used to detect target miRNA in the range from 10 fM to 10 nM).[14] Nevertheless, the use of excessive SP with expensive labels greatly increased the cost and may lead to false positive signals due to nonspecific adsorptions.[16-17]

To meet the challenge, we design herein a locker strand to stabilize the target miR and prevent it from forming silent CP/miR site, thus eliminating the risk of above mentioned false negative signals (case 3, Figure 1). In this work, we have used a fiber based fluorescent DNA sensing platform to demonstrate this free-energy-driven lock/open assembly based sensing strategy.[18] CPs were covalently modified onto the fiber surface, and Cy5.5 fluorophore labeled DNAs were adopted as SPs. In particular, Hsa *let-7a* was selected as the model target due to its implication in cancerous

diagnosis[19]: As an important MYC oncogene regulating miR, *let-7a* was reported to be aberrant expressed in various cancers, including breast cancer,[20] colon cancer,[21] lung cancer[22] and others.[23] After sensing surface preparation, thermodynamic criteria in design of the locker strand were discussed. False negative signals were effectively suppressed using the free-energy-driven dynamic lock/open DNA assembly based sensing strategy. The high sensitivity of the optical DNA biosensor allows for the detection of target miR at a concentration as low as 24 pM with a short TTR (≤4 min). *Let-7a* levels in urine and serum samples could also be tested using the optical DNA sensor, demonstrating the applicability of the free-energy-driven lock/open assembly based sensing strategy for clinical monitoring of miR levels for cancer prognosis and diagnosis.

Experimental section

Materials. Quartz optical-fiber with a length of 8.5 cm and a diameter of 600 μm was purchased from Chunhui Science & Technology Industrial Co., China. Glutaraldehyde (25% aqueous solution), 3-aminopropyl-triethoxysilane (APTS), bovine serum albumin (BSA), sodium citrate ($Na_3C_5H_5O_7 \cdot 3H_2O$), citric acid ($C_6H_8O_7 \cdot H_2O$), sodium chloride, Tris-HCl and formamide were purchased from Sigma-Aldrich, Inc, USA. Glycine and sodium cyanoborohydride ($NaCNBH_3$) were purchased from AMRESCO LLC. RNA Lysis buffer was purchased from Promega (Z3051). Tetramethyl ammonium chloride (TMAC) were bought from Beijing J&K Chemical company. Trichloroacetic acid (TCA) was bought from Innochem. Human serum was bought from Genia Biotech. Acetonitrile was bought from Fisher Scientific. All acids and other organic solvents were purchased from Beijing Chemical Works. All aqueous solutions were prepared using molecular biology grade USP sterile purified water (Corning Cellgro, NY, USA). All DNA and RNA

oligonucleotides (HPLC-purified) were purchased from Sangon Biotechnology Co. Ltd. (Shanghai, China), as listed in Table 1.

Table 1 DNA/RNA sequences used in this work

Name	Type	Sequence (5′-3′)
PolyA10	DNA	NH_2-$(CH_2)_6$-AAAAAAAAAA
CP	DNA	NH_2-$(CH_2)_6$-AAAAAATTAACTATACAA
SP	DNA	CCTACTACCTCAAAAAA-Cy5.5
Locker	DNA	AACTATGGGGGCAACCTA
let-7a	RNA	UGAGGUAGUAGGUUGUAUAGUU

Buffers Equilibration buffer: 10 mM PBS buffer, pH 7.4 (diluted from Phosphate Saline Packs, Thermo Company); Hybridization buffer: 10 mM Tris-HCl, 0.25 M $MgCl_2$, 0.1% tween-20, pH 7.9; SSC buffer: 20X SSC/40% formamide/3 M TMAC; Washing buffer: 0.05% SDS, pH 1.9.

Preparation of CP immobilized fiber surface

Briefly, amino modified CP strands were immobilized on the fiber surface using 3-aminopropyl-triethoxysilane (APTS) and glutaraldehyde as linkers according to the previously reported method (Figure 2c).[18] Firstly, optical-fiber with a tapered strucure was obtained through HF etching. The optical-fiber diameter was monitored with a microelectrode polisher (model 2002-C, Inbio Life Science Instrument Co., Ltd., Hubei, China). As shown in Figure 2c, the sensing surface generation procedure included four consecutive treatments: (1) An opfical-fiber with tarpered-structure was immersed in hot piranha solution (3:1 mixture of H_2SO_4 and 30% H_2O_2) for 1 h at 110 ^oC to generate a hydroxyl-activated surface (Please note that piranha solution is strongly oxidizing and should be carefully handled in open glasswares) and thoroughly washed with water and dried with a stream of N_2; (2) The hydroxyl-activated optical-fiber was modified with a ATPS layer using 1% v/v APTS in dry toluene for 2 h at room temperature. Afterwards, the optical-fiber

was cleaned in toluene and further fixed at 200 ^{o}C for 1 h; (3) An aldehyde-actived surface was achieved by immersing the optical-fiber was in 1% v/v glutaraldehyde (GA) aqueous solution overnight using a 37 ^{o}C shaker; (4) Capture probes (CPs) with amino modified 6-carbon linkers on their 5' end, were immobilized to the sensing surface by immersing the optical-fiber in 100 nM of CP and 100 nM of polyA10 (as a short mixer) in 50 mM NaCl aqueous solution for 1 h at 37 ^{o}C with gentle shaking. Excess aldehyde groups were blocked by 20 mM glycine aqueous solution for 1 h at room temperature. Next, the optical-fiber was reduced in 20 mg/mL of $NaCNBH_3$ aqueous solution for 1h. Finally, the optical-fiber was blocked with 2 mg/mL of isoelectric BSA for more than 6 hours to reduce nonspecific adsorption.[18]

MiR detection in buffer, urine and serum

For all miR detections in buffer, the concentrations of SP and locker were fixed at 5 nM and 20 nM, respectively. Different concentrations of target miR (1 pM-15 nM) were prepared in hybridization buffer containing SP and locker. The obtained mixtures were first incubated in a 90 ^{o}C water bath for 3 min, then incubated at room temperature (r.t.) for another 3 min (all reaction vials were wrapped in foil). The obtained mixtures were directly pumped into the flow cell of the DNA sensor for evanescent wave induced fluorescent measurement.

For miR detection in human urine, 0.01% v/v of RNA lysis buffer was added into freshly collected urine samples and the mixtures were sufficiently mixed. Next, urine samples from healthy donors spiked with different *let-7a* concentrations were diluted 10 times using 20X SSC buffer. Then the diluted solutions were supplemented with 5 nM SP and 20 nM locker. The obtained mixtures were

first incubated in a 90 ºC water bath for 3 min, then incubated at r.t. for another 3 min before evanescent wave induced fluorescent measurement using the DNA sensor.

For miR detection in human serum, 200 μL of serum was mixed with 1.5 mL of 10% TCA and 300 μL of acetonitrile, and then the obtained mixture was centrifuged at 12, 000 rpm for 15 min at 4ºC. The obtained supernatant (spiked with *let-7a*) were diluted 10 times using 100 mM PBS buffer. Then the diluted solution was supplemented with 5 nM SP and 20 nM locker, and was incubated at r.t. for 3 min before evanescent wave induced fluorescent measurement using the DNA sensor.

Results and Discussion

The fiber based fluorescent DNA sensor

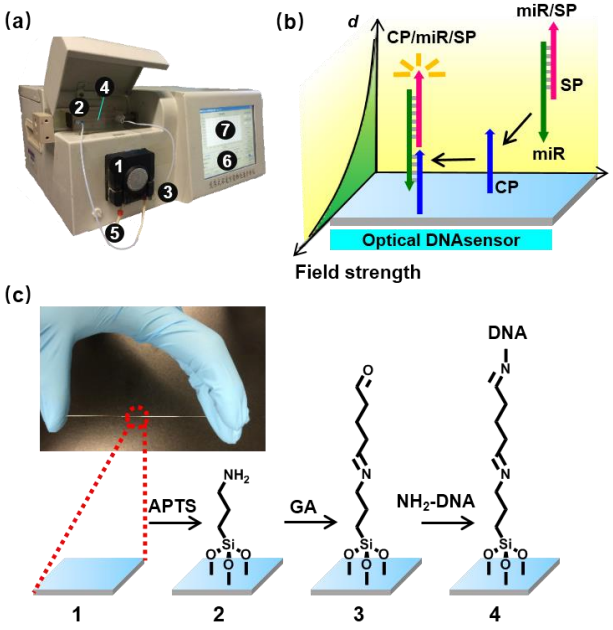

Figure 2. (a) Photograph of the fiber based DNA sensor developed by our group. Key parts for regular users include ① pump, ② flow cell, ③ sample inlet, ④ optical-fiber, ⑤ waste outlet, ⑥ control panel and ⑦ signal window. (b) Schematic illustration of the surface involved sandwich assay for detection of target miRNA. (c) DNA step-by-step immobilization onto the fiber sensing surface: Bare saline surface (1), ammino functionalized surface (2), glutaralderhyde actived surface (3) and DNA covalently immobilized surface (4).

A homemade fiber based fluorescent DNA sensor (Figure 2a) was used to demonstrate this free-energy-driven lock/open assembly based sensing strategy, and was further used for cancer-related miR detection in urine samples. Briefly, an exponential decayed evanescent field (usually half of wavelength of incident light from the fiber's surface) formed around the fiber surface, as shown in Figure 2b. After forming a CP/miR/SP sandwich structure by hybridization, fluorophores labeled on SP would be excited within the evanescent field. By measuring the fluorescence emission, the amount of target miR could be directly observed using the DNA sensor. One typical sensorgram is comprised of 4 stages, as shown in Figure S1.

Design of the lock/open DNA assembly based strategy

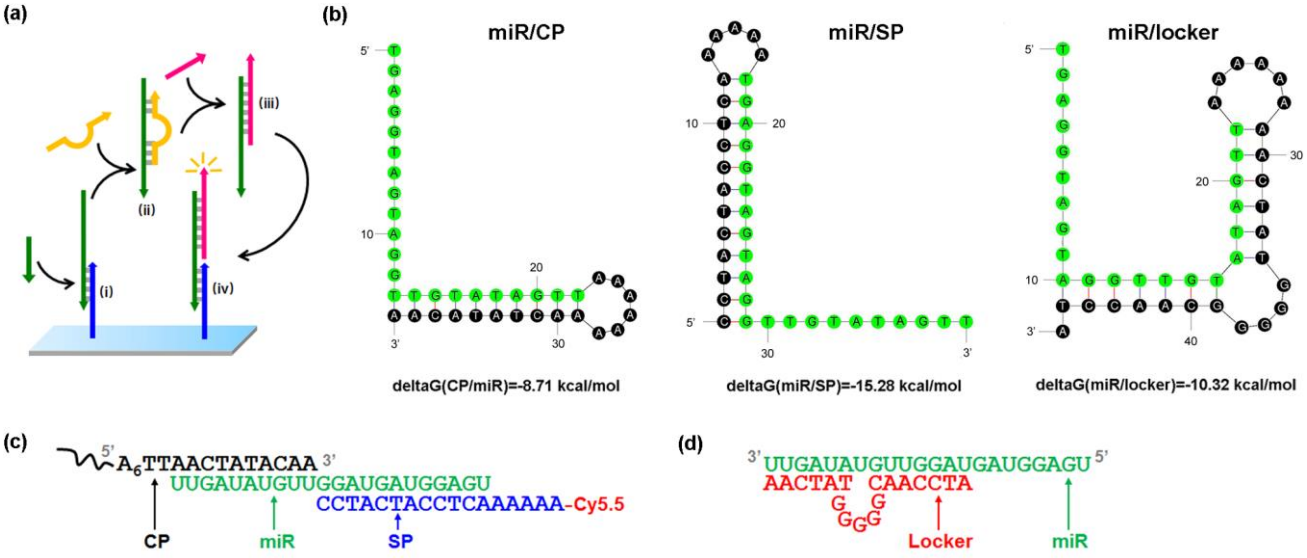

Figure 3. (a) Schematic illustration of the stepwise details of a free-energy-driven lock/open assembly switching system realized by a locker. The locker is plotted in yellow. (i) CP/miR, (ii) miR/locker, the lock assembly, (iii) miR/SP, the open assembly, (iv) CP/miR/SP, the sandwich assembly. (b) Secondary structures of CP/miR, miR/SP and miR/locker predicted by the mfold web server (folding at 25 °C, 1.0 M Na^+). The DNA sequence corresponding to miR *let-7a* (highlighted in green) is linked with CP, SP or locker sequence by six A nucleotides. (c) Structure of CP/miR/SP sandwich assay. (d) Structure of miR/locker complex.

As described in the introduction part, one key challenge for a SST biosensor is the existence of false negative signals when target miR are more than SP in solution phase (Figure 1, case 2). In that case, if a sample contains miR and miR/SP at the same time, they would compete for limited surface hybridization sites. Usually, the concentration of fluorescent labeled SP is fixed for a well-developed assay, thus the increased ratio of target miR in the sample would decrease the hybridization percentage of miR/SP, turning the signal off (false negative signals).

Due to the highly specific interactions between complementary nucleotides, DNA could act as a powerful construction material by design of its sequence.[24] One way to avoid above mentioned false negative signals is to rationally program miR/SP assembly pathway, which could be encoded into nucleic acid sequences.[25] Inspired by DNA-fueled free-running DNA nanomachines,[26] a dynamic lock/open DNA assembly based sensing strategy realized by a locker sequence was designed as shown in Figure 1, case 3. Stepwise details of the strategy were illustrated in Figure 3a. Design of the locker strand is based on the following considerations: First, the lock assembly (miR/locker, Figure 3a-ii) should provide moderate thermodynamic stability in the system, preventing miR from generating silent CP/miR sites (Figure 3a-i). Second, in the presence of SP, lock assembly would switch to open assembly (miR/SP, Figure 3a-iii), which could further hybridize with the immobilized CP, forming a stable sandwich structure (CP/miR/SP, Figure 3a-iv). Finally, based on the discovery that competing DNA is thermodynamically favored to displace a shorter DNA strand[27] and that decreasing the length of DNA duplex could speed up the rate of strand exchange reactions drastically,[28] a locker strand with two short binding arms and a central bulge is preferable to a short linear DNA for easier strand displacement and more complete strand replacement. Based on these

considerations, the switching between lock assembly and open assembly should be free-energy-driven, and the locker served as a temporary reservoir for target miRs, preventing free miRs from generating silent CP/miR sites.

As shown in Figure 3b, by linking the DNA sequence corresponding to miR (highlighted in green) with CP, SP or locker sequence by six A nucleotides, the secondary structures as well as thermodynamic parameters of CP/miR, miR/SP and miR/locker could be *in silico* predicted by the mfold web server.[29] Different locker sequences would form secondary structures with varied free energies. According to the considerations about the locker design, free energies of three assemblies in the system should meet the requirement that deltaG(miR/SP) < deltaG(miR/locker) < deltaG(CP/miR) < 0. A miR/18 nt sequence (AACTATGGGGGCAACCTA) is found to form an expected secondary structure with a free energy of -10.32 kcal/mol, lying within the free energy range between miR/SP (-15.28 kcal/mol) and CP/miR (-8.71 kcal/mol), while other designed candidate sequences would not meet such free energy criterion. Therefore, the 18 nt sequence was used as the locker in the following study.

Suppression of false negative signals using the lock/open assembly based strategy

First of all, false negative signals generated on the fiber based fluorescent SST DNA sensor were characterized. In our system, both CP and SP are designed to hybridize with the 22-mer target miR (*let-7a*) from both 3′ and 5′ ends, forming 10 and 12 base pairs, respectively (see Figure 3c for the specific sequences). When the concentration of SP is fixed at 5 nM, the increase of miR concentration led to a volcano shaped calibration curve with a peak observed at the equivalent point (c(miR)=c(SP)=5 nM, Figure 4a). The decreased signals after equivalent point were so called “false

negative signals" as above mentioned. Similar phenomena also appeared when the concentration of SP was fixed at 2.5 nM and 10 nM (Figure S3).

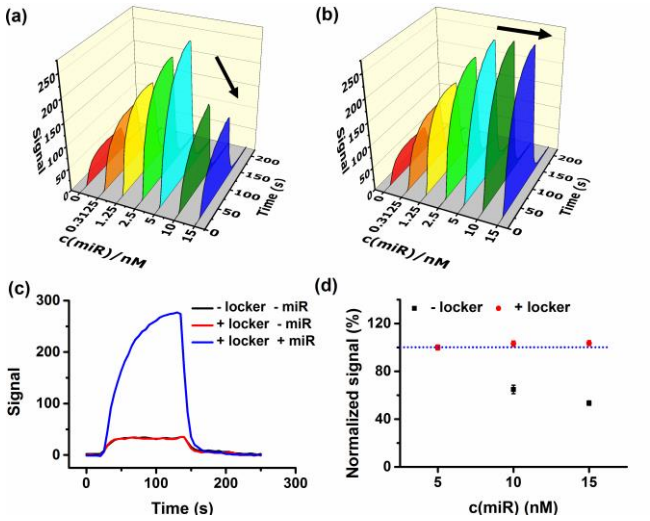

Figure 4. Sensorgrams of the CP/miR/SP sandwich assays induced by different concentrations of miR with (a) or without (b) adding the locker strand. Experiments were performed in hybridization buffer containing 5 nM of SP. (c) Sensorgrams of three CP/miR/SP sandwich assays. Black curve: 5 nM SP only; Red curve: 5 nM SP, 20 nM locker strand; Blue curve: 5 nM SP, 5 nM miR and 20 nM locker strand. (d) Normalized signals of the CP/miR/SP sandwich assays induced by 5, 10 and 15 nM of miR with (red dots) or without (black dots) the addition of locker.

Next, we evaluated the effect of adding the locker into the detection system using the fiber based fluorescent SST DNA sensor. Specific sequences and the structure formed by the miR/locker complex were plotted in Figure 3d. First of all, in the absence of target miR, *let-7a*, 5 nM SP in hybridization buffer led to a slightly signal increase due to its diffusion in homogeneous phase or a small extent of nonspecific adsorption (Figure 4c, black curve). The addition of 20 nM locker into 5 nM of SP almost showed no effect on the signal amplitude (Figure 4c, red curve). In contrast, in the same system with 20 nM locker and 5 nM of SP, a progressive increase in the signal was apparent in the presence of 5 nM of target miR (Figure 4c, blue curve). This indicated that SP would effectively hybridize with miR and immobilized CP by forming the sandwich structure. In the system with

locker added, when the concentration of miR exceeded SP, a plateau stage instead of the volcano shaped calibration curve was observed (Figure 4b). By designating signal induced by 5 nM miR as 100%, normalized signals of the CP/miR/SP sandwich assays induced by 5, 10 and 15 nM of miR with or without the addition of locker were plotted in Figure 4d. Obviously, false negative signals were effectively suppressed using this lock/open assembly based sensing strategy.

MiR detection in buffer using the lock/open assembly based strategy

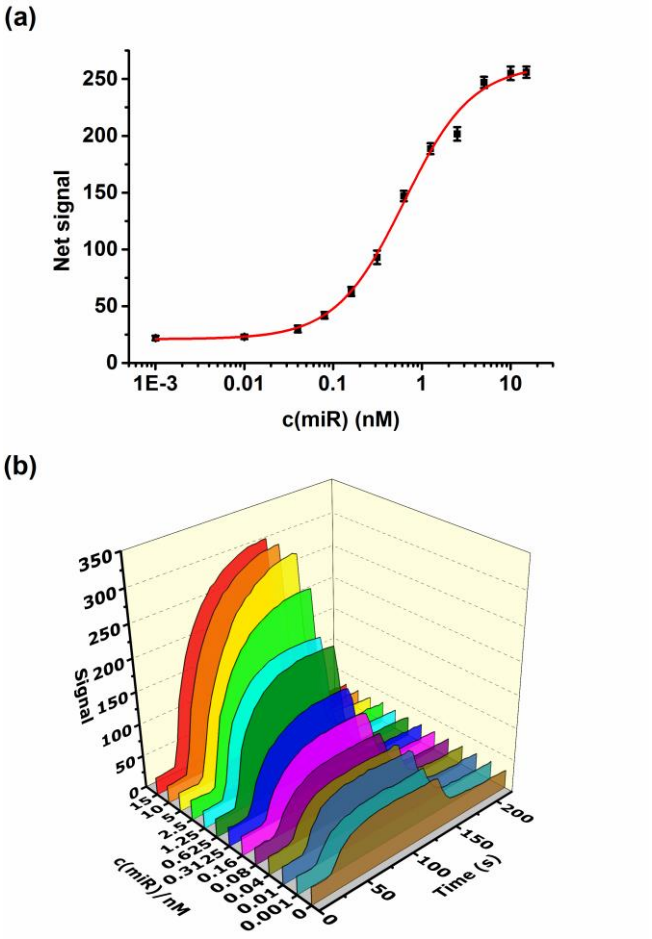

Figure 5. Detection performances of the DNA sensor for target miR. (a) Variations of net signals with different miR concentrations (1 pM-15 nM) and the corresponding four-parameter logarithmic fitted calibration plot. (b) Original sensorgrams of the CP/miR/SP sandwich assays generated in the presence of different concentrations of miR (1 pM-15 nM) without deducting the baseline.

As described in experimental section, the two-step switching between lock assembly and open assembly was simplified to a one-step operation in detecting miR *let-7a* in buffer. Samples

containing target miR at different concentrations (1 pM-15 nM) were tested using the DNA sensor. Four-parameter logistic fit of the net signals obtained from this free-energy-driven lock/open assembly based optical DNA sensor was plotted in Figure 5a as a calibration curve for target miR. Original sensorgrams corresponding to the calibration curve were shown in Figure 5b. The detection limit (LOD) was calculated to be 24 pM (EC10 of the logistic model). It should be noted that detection performances (especially the upper detection range) of such DNA immobilized SST biosensors are correlated to the surface CP density as well as SP concentration used, which could be further optimized as needed. One interesting point to note is that, from the aspect of equilibrium partition, the locker may also serve as a reservoir for miR in non-excess case. Therefore, miR sensing performances using the developed DNA sensor with/without the addition of locker is compared (Figure S4). In general, larger slope obtained from linear fitting represents higher sensitivity. The slopes of experimental groups with or without the addition of locker are 0.47 and 0.49, respectively (Figure S4(b)). The small difference (4%) suggested that the influence of this reservoir effect on sensitivity is quite small. Theoretically, since deltaG(miR/SP)= −15.28 kcal/mol < deltaG(miR/locker) = −10.32 kcal/mol, it is very possible that the amount miR/locker is negligible compared with miR/SP.

MiR detection in urine and serum samples using the lock/open assembly based strategy

Considering that urine provides many biomarkers in a noninvasive way, it serves as a useful matrix for clinical detection.[30] In detecting miR in urine, a small amount of lysis buffer containing guanidinium thiocyanate was added to collected urine samples in order to inhibit RNase activity and prevent RNA from degradation.[31] Besides, the feasibility of miR detection in another frequently used

sample, human serum, was also investigated using this developed DNA sensor. In standard tests, spiked miR in both urine and serum samples could be detected with recovery rates higher than 75% (Figure 6). And the developed DNA sensor is sensitive enough to reflect signal changes caused by small RNA concentration fluctuation. Since the abnormal expression of miRs has been reported in many types of cancers, this lock/open assembly based DNA sensor could serve as a useful tool in diagnostic applications.

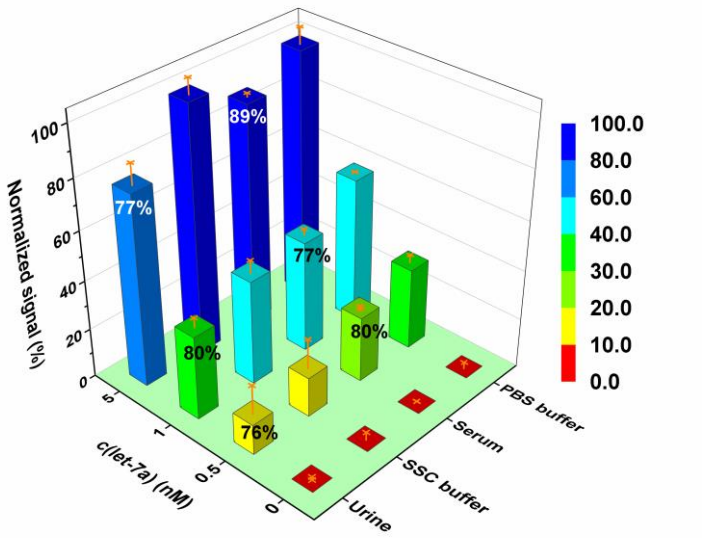

Figure 6 MiR detection in urine and serum samples using the lock/open assembly based strategy. Corresponding recovery rates are labeled in this figure.

Conclusions

In conclusion, we have applied a free-energy-driven dynamic lock/open DNA assembly for highly sensitive fluorescent detection of miR *let-7a* based on a sandwich-type biosensor using two DNA probes (SP and CP). Fluorescent labeled SP tends to be trapped within the evanescent field through the formation of sandwich-type SP/miRNA/CP structure, thereby turning the signal on. This turn-on process enables the detection of target miR in concentrations as low as 24 pM in less than 4 min. Moreover, the applicability of this free-energy-driven lock/open assembly based optical DNA sensor

was demonstrated using human urine and serum samples (recovery rates>75%). Significantly, the sensing performances of this free-energy-driven lock/open assembly based optical DNA sensor may be further adjusted by simply changing the amount of SP as needed. We believe that this work will provide inspiration for relative researches, and may widen the application of DNA nanomachine as a potent tool in the field of biosensing as well as surface-related research.

Associated Content

Supporting Information. Data processing of the DNA sensor and all supplementary figures supplied as Supporting Information (PDF file).

Author Information

Corresponding Author

* E-mail: xhzhou@mail.tsinghua.edu.cn.

Author Contributions

[§]Xiyu Zhu and Ruoyu Wang contributed equally to this work and should be considered as co-first authors.

All authors have given approval to the final version of the manuscript.

Notes

The authors declare no competing financial interest.

Funding Sources

This research is supported by the National Nature Science Foundation of China (21677082).

References

1. Bohunicky, B.; Mousa, S. A., Biosensors: The New Wave in Cancer Diagnosis. *Nanotechnol. Sci. Appl.* **2010,** *4*, 1-10.

2. Pereira, D. M.; Rodrigues, P. M.; Borralho, P. M.; Rodrigues, C. M. P., Delivering the Promise of MiRNA Cancer Therapeutics. *Drug Discovery Today* **2013,** *18*, 282-289.
3. Xie, B.; Ding, Q.; Han, H.; Wu, D., MiRCancer: A MicroRNA–Cancer Association Database Constructed by Text Mining on Literature. *Bioinformatics* **2013,** *29*, 638-644.
4. Johnson, B. N.; Mutharasan, R., Biosensor-Based MicroRNA Detection: Techniques, Design, Performance, and Challenges. *The Analyst* **2014,** *139*, 1576-1588.
5. Zhai, Q.; He, Y.; Li, X.; Guo, J.; Li, S.; Yi, G., A Simple and Ultrasensitive Electrochemical Biosensor for Detection of MicroRNA Based on Hybridization Chain Reaction Amplification. *J. Electroanal. Chem.* **2015,** *758*, 20-25.
6. Šípová, H.; Zhang, S.; Dudley, A. e. M.; Galas, D.; Wang, K.; Homola, J. i., Surface Plasmon Resonance Biosensor for Rapid Label-Free Detection of Microribonucleic Acid at Subfemtomole Level. *Anal Chem* **2010,** *82*, 10110-10115.
7. Qavi, A. J.; Bailey, R. C., Multiplexed Detection and Label-Free Quantitation of MicroRNAs using Arrays of Silicon Photonic Microring Resonators. *Angew. Chem., Int. Ed.* **2010,** *49*, 4608-4611.
8. Zhang, G.-J.; Chua, J. H.; Chee, R.-E.; Agarwal, A.; Wong, S. M., Label-Free Direct Detection of MiRNAs with Silicon Nanowire Biosensors. *Biosens. Bioelectron.* **2009,** *24*, 2504-2508.
9. He, L.; Musick, M. D.; Nicewarner, S. R.; Salinas, F. G.; Benkovic, S. J.; Natan, M. J.; Keating, C. D., Colloidal Au-Enhanced Surface Plasmon Resonance for Ultrasensitive Detection of DNA Hybridization. *J. Am. Chem. Soc.* **2000,** *122*, 9071-9077.
10. Seokheun, C.; Junseok, C., Methods of Reducing Non-Specific Adsorption in Microfluidic Biosensors. *J. Micromech. Microeng.* **2010,** *20*, 075015.
11. Wang, J.; Kawde, A.-N.; Erdem, A.; Salazar, M., Magnetic Bead-Based Label-Free Electrochemical Detection of DNA Hybridization. *The Analyst* **2001,** *126*, 2020-2024.
12. Engvall, E.; Perlmann, P., Enzyme-Linked Immunosorbent Assay (ELISA) Quantitative Assay of Immunoglobulin G. *Immunochemistry* **1971,** *8*, 871-874.
13. Gao, X.; Xu, H.; Baloda, M.; Gurung, A. S.; Xu, L.-P.; Wang, T.; Zhang, X.; Liu, G., Visual Detection of MicroRNA with Lateral Flow Nucleic Acid Biosensor. *Biosens. Bioelectron.* **2014,** *54*, 578-584.
14. Wen, Y.; Liu, G.; Pei, H.; Li, L.; Xu, Q.; Liang, W.; Li, Y.; Xu, L.; Ren, S.; Fan, C., DNA Nanostructure-Based Ultrasensitive Electrochemical MicroRNA Biosensor. *Methods* **2013,** *64*, 276-282.
15. Zhang, Y.; Zhang, C. Y., Sensitive Detection of MicroRNA with Isothermal Amplification and A Single-Quantum-Dot-Based Nanosensor. *Anal Chem* **2011,** *84*, 224-231.
16. Langer, R.; Tirrell, D. A., Designing Materials for Biology and Medicine. *Nature* **2004,** *428*, 487-492.
17. Mao, X.; Yang, L.; Su, X.-L.; Li, Y., A Nanoparticle Amplification Based Quartz Crystal Microbalance DNA Sensor for Detection of Escherichia Coli O157:H7. *Biosens. Bioelectron.* **2006,** *21*, 1178-1185.
18. Wang, R. Y.; Zhou, X. H.; Zhu, X. Y.; Yang, C.; Liu, L. H.; Shi, H. C., Isoelectric Bovine Serum Albumin: Robust Blocking Agent for Enhanced Performance in Optical-Fiber Based DNA Sensing. *ACS Sens.* **2017,** *2*, 257-262.

19. Sampson, V. B.; Rong, N. H.; Han, J.; Yang, Q.; Aris, V.; Soteropoulos, P.; Petrelli, N. J.; Dunn, S. P.; Krueger, L. J., MicroRNA Let-7a Down-Regulates MYC and Reverts MYC-Induced Growth in Burkitt Lymphoma Cells. *Cancer Res.* **2007,** *67*, 9762-9770.
20. Wang, L.; Wang, Y. X.; Zhang, D. Z.; Fang, X. J.; Sun, P. S.; Xue, H. C., Let-7a Mimic Attenuates CCL18 Induced Breast Cancer Cell Metastasis through Lin 28 Pathway. *Biomed. Pharmacother.* **2016,** *78*, 301-307.
21. Ogata-Kawata, H.; Izumiya, M.; Kurioka, D.; Honma, Y.; Yamada, Y.; Furuta, K.; Gunji, T.; Ohta, H.; Okamoto, H.; Sonoda, H.; Watanabe, M.; Nakagama, H.; Yokota, J.; Kohno, T.; Tsuchiya, N., Circulating Exosomal Micrornas as Biomarkers of Colon Cancer. *PLoS ONE* **2014,** *9*, e92921.
22. Karube, Y.; Tanaka, H.; Osada, H.; Tomida, S.; Tatematsu, Y.; Yanagisawa, K.; Yatabe, Y.; Takamizawa, J.; Miyoshi, S.; Mitsudomi, T.; Takahashi, T., Reduced Expression of Dicer Associated with Poor Prognosis in Lung Cancer Patients. *Cancer Sci.* **2005,** *96*, 111-115.
23. Boyerinas, B.; Park, S.-M.; Hau, A.; Murmann, A. E.; Peter, M. E., The Role of Let-7 in Cell Differentiation and Cancer. *Endocr.-Relat. Cancer* **2010,** *17*, F19-F36.
24. Yurke, B.; Turberfield, A. J.; Mills, A. P.; Simmel, F. C.; Neumann, J. L., A DNA-Fuelled Molecular Machine Made of DNA. *Nature* **2000,** *406*, 605-608.
25. Yin, P.; Choi, H. M. T.; Calvert, C. R.; Pierce, N. A., Programming Biomolecular Self-Assembly Pathways. *Nature* **2008,** *451*, 318-322.
26. Bath, J.; Turberfield, A. J., DNA Nanomachines. *Nat. Nano.* **2007,** *2*, 275-284.
27. Li, F.; Zhang, H.; Wang, Z.; Li, X.; Li, X.-F.; Le, X. C., Dynamic DNA Assemblies Mediated by Binding-Induced DNA Strand Displacement. *J. Am. Chem. Soc.* **2013,** *135*, 2443-2446.
28. Reynaldo, L. P.; Vologodskii, A. V.; Neri, B. P.; Lyamichev, V. I., The Kinetics of Oligonucleotide Replacements. *J. Mol. Biol.* **2000,** *297*, 511-520.
29. Zuker, M., Mfold Web Server for Nucleic Acid Folding and Hybridization Prediction. *Nucleic Acids Res.* **2003,** *31*, 3406-3415.
30. Royo, F.; Diwan, I.; Tackett, M.; Zuñiga, P.; Sanchez-Mosquera, P.; Loizaga-Iriarte, A.; Ugalde-Olano, A.; Lacasa, I.; Perez, A.; Unda, M.; Carracedo, A.; Falcon-Perez, J., Comparative MiRNA Analysis of Urine Extracellular Vesicles Isolated through Five Different Methods. *Cancers* **2016,** *8*, 112.
31. Peng, J.; Xia, Z.; Chen, L.; Shi, M.; Pu, J.; Guo, J.; Fan, Z., Rapid and Efficient Isolation of High-Quality Small RNAs from Recalcitrant Plant Species Rich in Polyphenols and Polysaccharides. *PLoS ONE* **2014,** *9*, e95687.

For TOC only

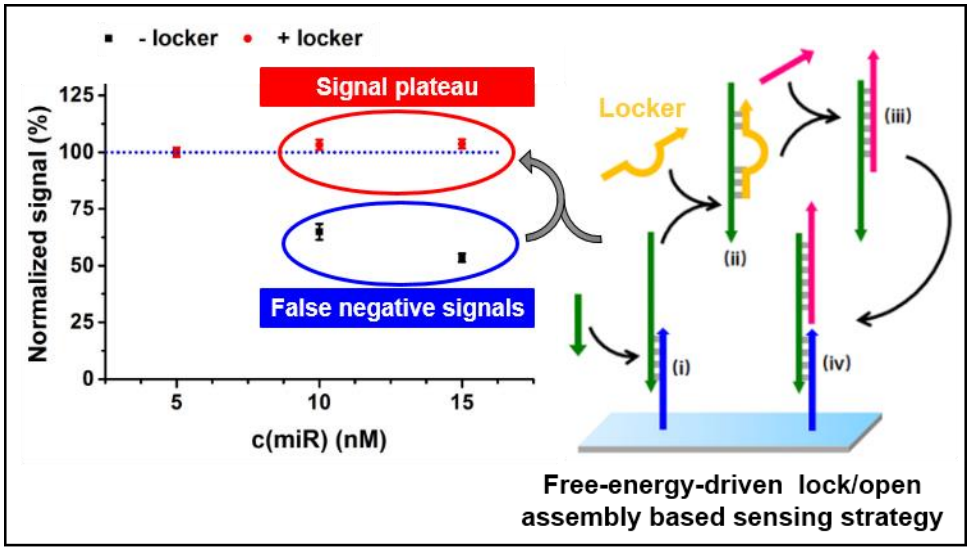
- locker
+ locker
Signal plateau
False negative signals
Normalized signal (%)
125
100
75
50
25
0
5
10
15
c(miR) (nM)
Locker
(i)
(ii)
(iii)
(iv)
Free-energy-driven lock/open assembly based sensing strategy